JOURNAL OF THE AMERICAN CHEMICAL SOCIETY
pubs.acs.org/JACS
Article

Fluorous Soluble Cyanine Dyes for Visualizing Perfluorocarbons in Living Systems

Irene Lim, Antoine Vian, Heidi L. van de Wouw, Rachael A. Day, Carlos Gomez, Yucen Liu, Arnold L. Rheingold, Otger Campàs,* and Ellen M. Sletten*

Liu Wenjuan

2020.09.17

Ellen M. Sletten

Assistant Professor
John McTague Career Development Chair
Department of Chemistry and Biochemistry
University of California, Los Angeles

- BS in Chemistry, 2006, Stonehill College, synthesis of alkaloid glycosidase inhibitors
- PhD in Chemistry, 2011, University of California, Berkeley, optimization and development of bioorthogonal chemistries and their subsequent applications in labeling living systems
- NIH Postdoctoral Fellow, 2011, Massachusetts Institute of Technology, with soft fluorous materials for use in fluorescent sensors
- Assistant Professor, 2015, Department of Chemistry and Biochemistry at UCLA

Research Interests

Fluorinated materials in diagnostic and therapeutic technologies development: organic synthesis, fluorous chemistry, chemical biology, nanoscience, supramolecular chemistry, polymer synthesis, photophysics and pharmacology.

FLUOROUS NANOTHERAPEUTICS

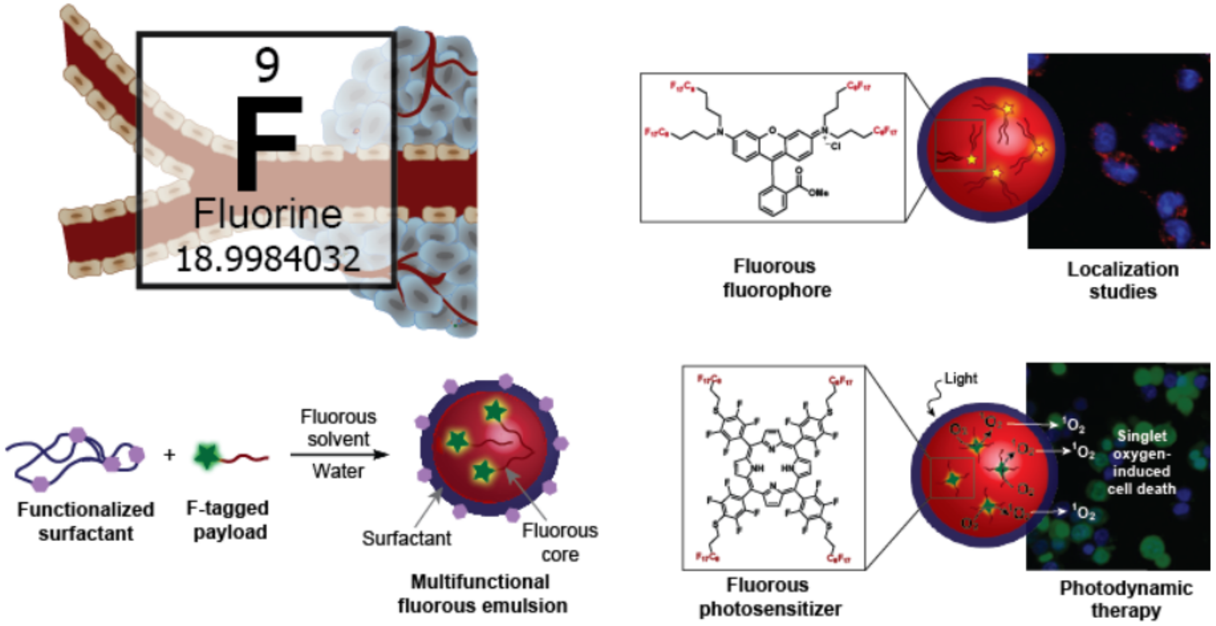

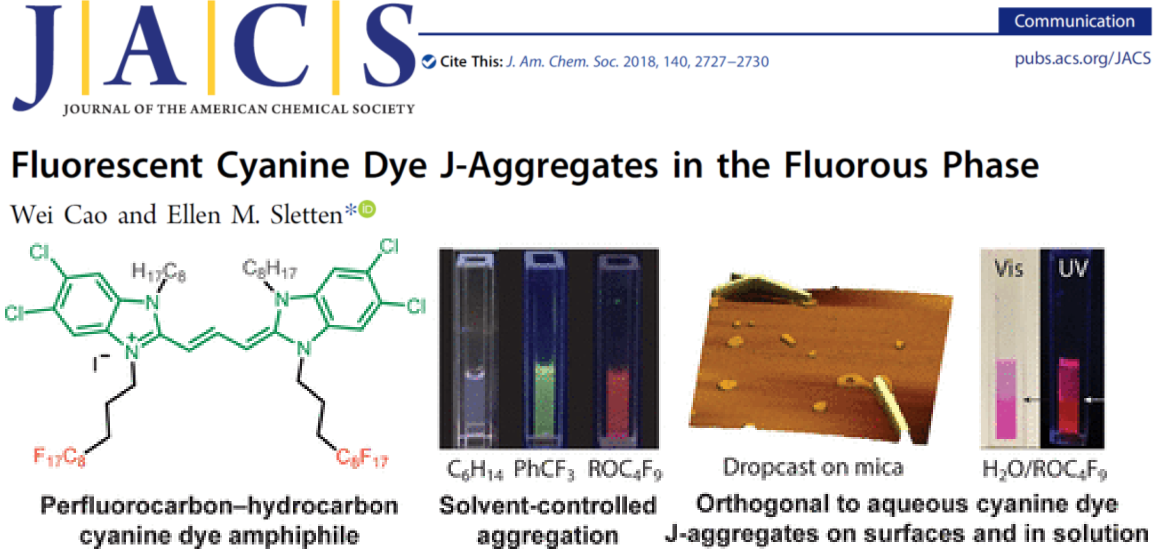

SHORTWAVE INFRARED DIAGNOSTICS

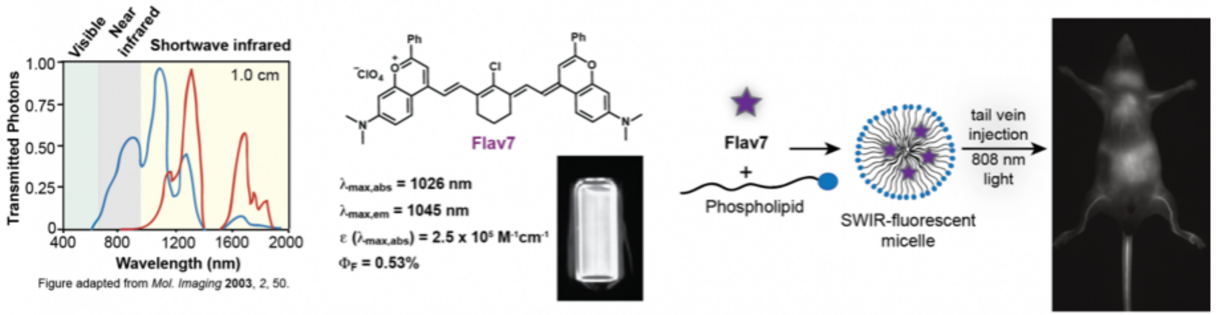

Optical imaging is a safe, cost-effective imaging modality, which can be readily multiplexed or engineered to have a turn-on response. Despite these advantages, optical imaging is not readily employed in the clinic due to the poor penetration of light through tissue and high background signal from endogenous chromophores. The shortwave infrared region of the electromagnetic spectrum has emerged as an optimal region for optical imaging due to the decreased scattering of light by tissue and minimal autofluorescence of endogenous biomolecules in this region. The potential of this region has been showcased using carbon nanotubes and quantum dots. Our group is developing non-toxic, small molecule fluorophores for this region.

A. The orthogonality of the fluorous phase

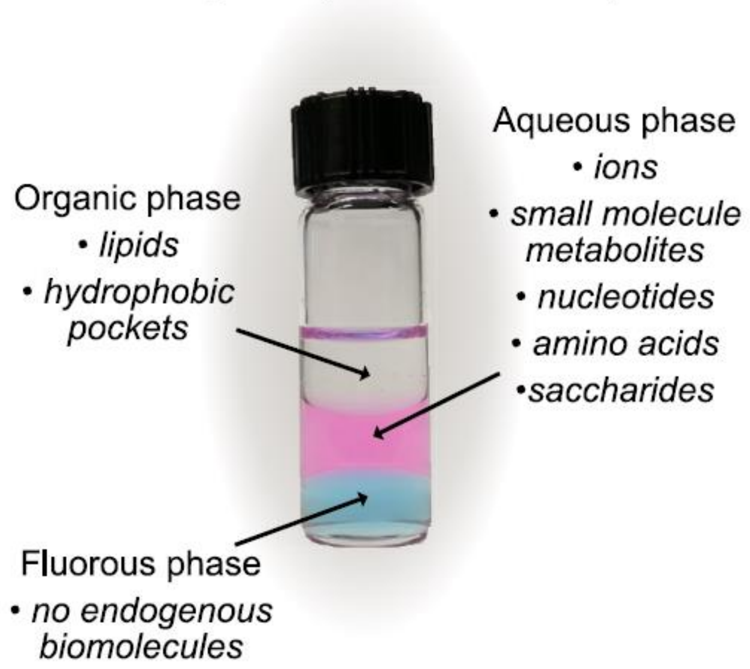

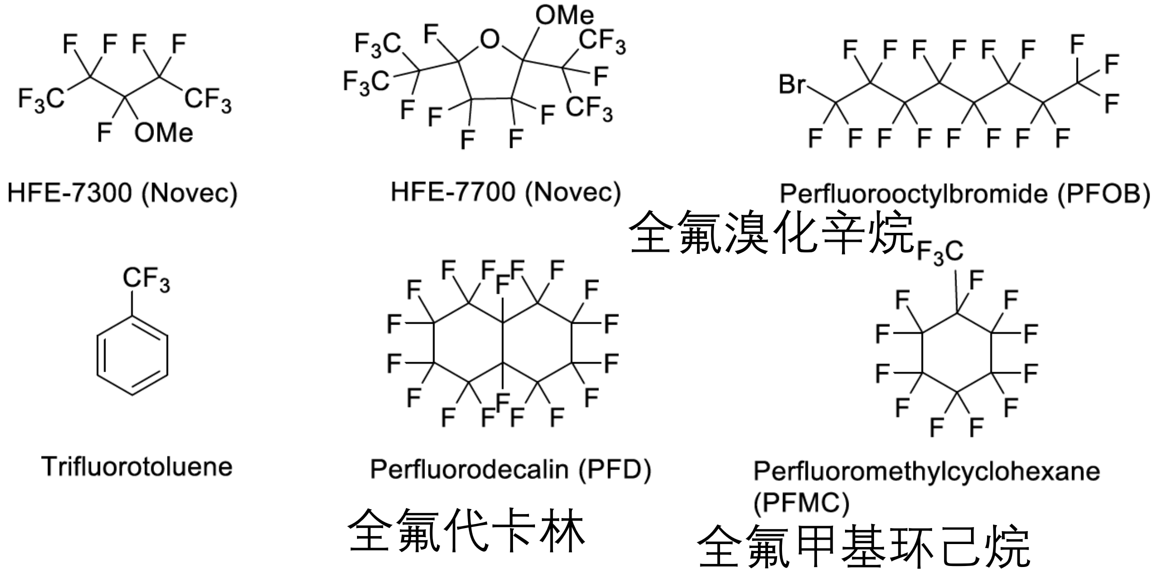

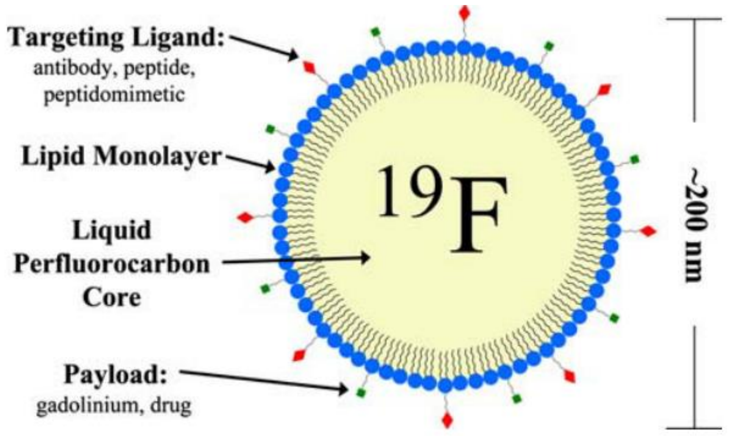

FIGURE 1. A schematic representation of a multifunctional liquid perfluorocarbon nanoemulsion. The liquid perfluorocarbon core is surrounded by a lipid monolayer which can be functionalized with targeting ligands and other payload. Additionally, drugs can be dissolved in the lipid layer or carried in the particle interior.

- ✓ microarray assembly
- ✓ antibiofouling coatings
- ✓ oxygen delivery
- ✓ ultrasound and magnetic resonance imaging diagnostics
- ✓ in vivo force measurements

A. Comparing hydrogen and fluorine nuclei

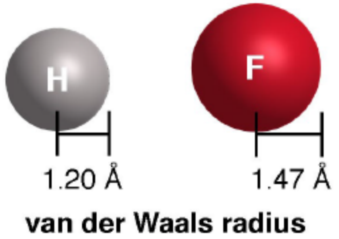

	H	F
electronegativity (Pauling)	2.1	4.0
polarizability ($x10^{-24}$ cm^3)	0.557	0.667

B. Comparing carbon bound to hydrogen vs. fluorine

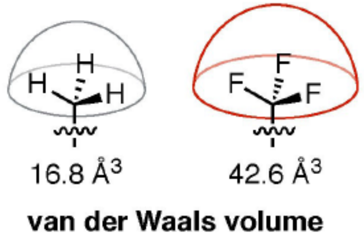

	C–H	C–F
dipole	⟵+	+⟶
bond length (Å)	1.09	1.35
bond strength (kcal/mol)	~105	~115

C. Comparing hydrocarbons and perfluorocarbons

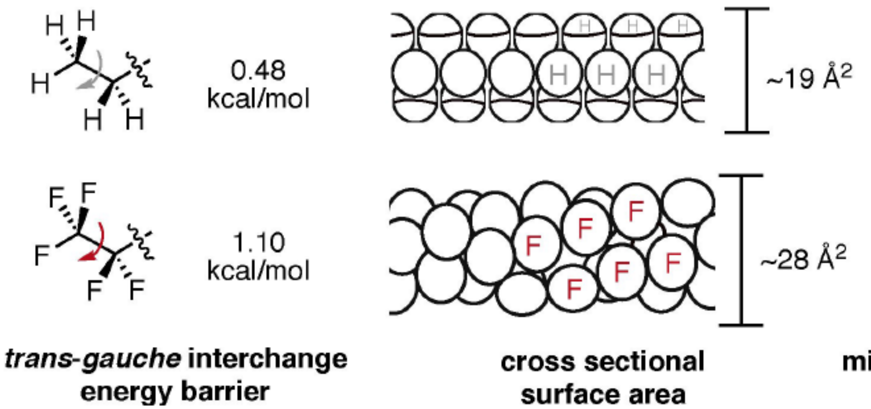

	BP (°C)
C_6H_{14}	68
C_6F_{14}	56

minimal intermolecular forces

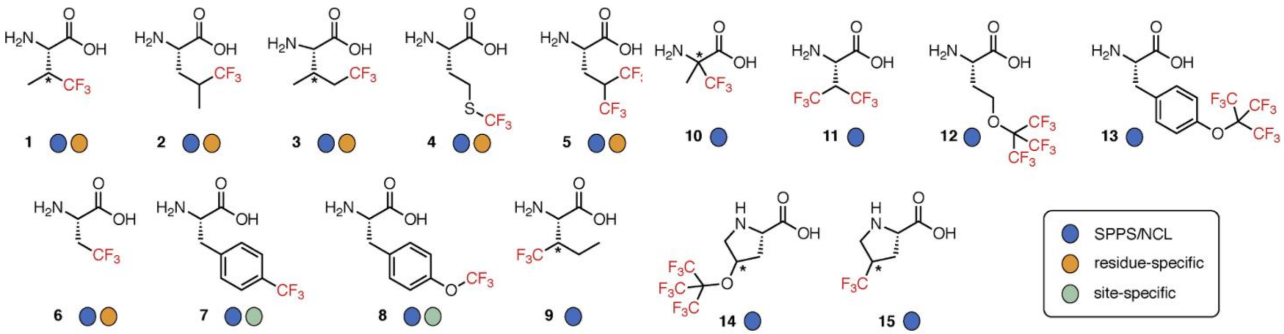

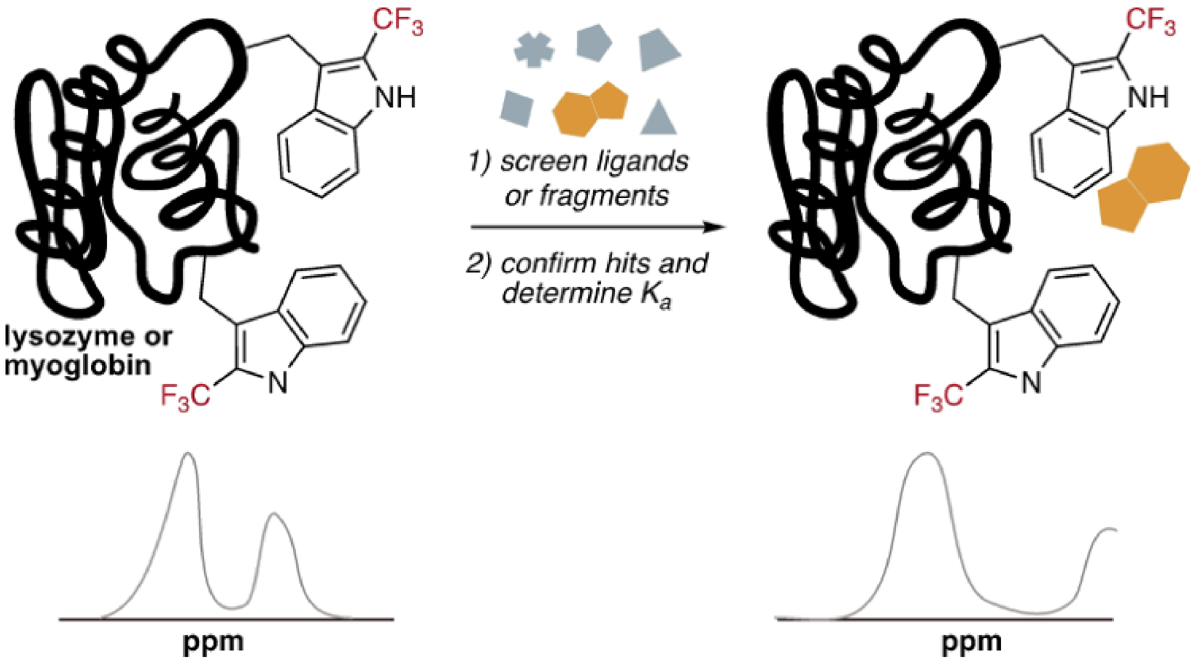

Figure 4. Protein-observed ^{19}F NMR (PrOF NMR). This method uses the incorporation of fluorinated amino acids to monitor protein conformation changes in the presence of small-molecule fragments for drug discovery. Proteins with trifluoromethylated tryptophan residues have been used in these types of studies.[72]

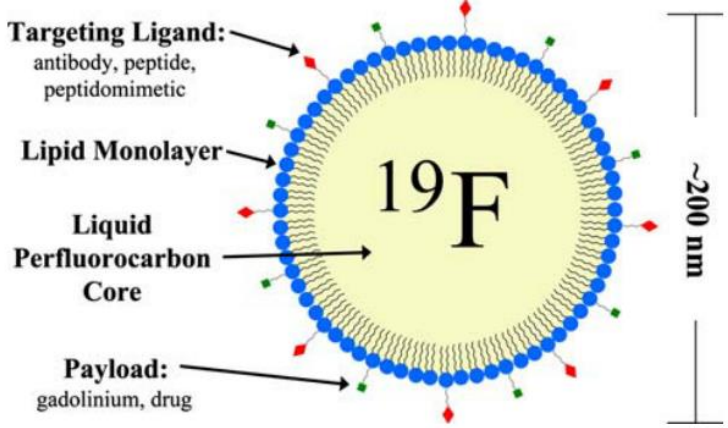

FIGURE 1. A schematic representation of a multifunctional liquid perfluorocarbon nanoemulsion. The liquid perfluorocarbon core is surrounded by a lipid monolayer which can be functionalized with targeting ligands and other payload. Additionally, drugs can be dissolved in the lipid layer or carried in the particle interior.

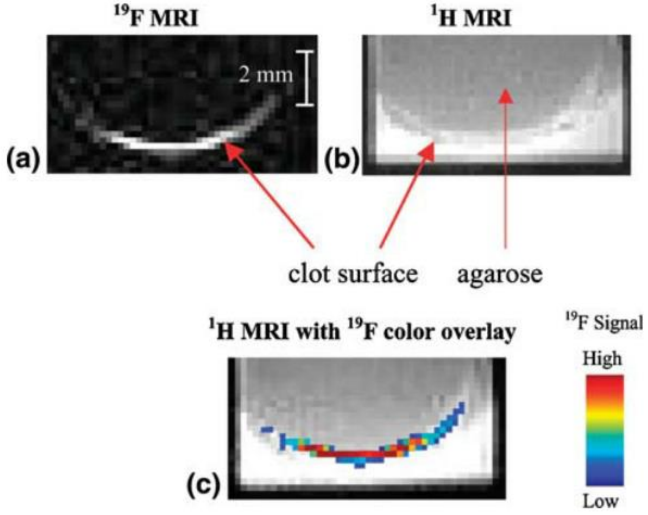

FIGURE 2. (a) ^{19}F image (4.7 T) of a single slice through a clot *in vitro* treated with fibrin-targeted crown ether emulsion. High signal is observed at the clot surface due to bound fluorinated nanoparticles. (b) ^{1}H image (4.7 T) of the same slice showing the anatomy of the clot with significant background ^{1}H signal. (c) False color overlay of ^{19}F signal onto ^{1}H image clearly localizing ^{19}F signal to clot surface. (Reprinted with permission from Morawski *et al.*[34])

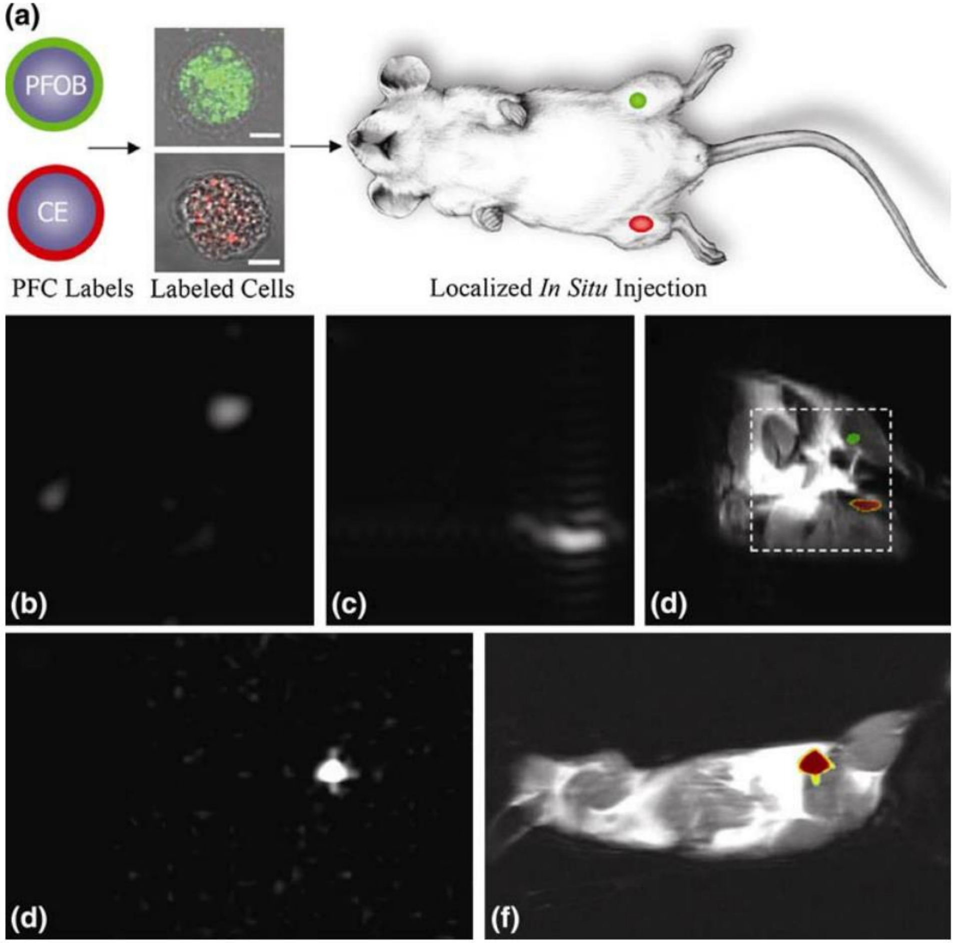

FIGURE 5. Localization of labeled cells after *in situ* injection. (a) To determine the utility for cell tracking stem/progenitor cells labeled with either PFOB (green) or CE (red), nanoparticles were locally injected into mouse thigh skeletal muscle. (b–d) At 11.7 T, spectral discrimination permits imaging the fluorine signal attributable to ~1 × 106 PFOB-loaded (b) or CE-loaded cells (c) individually, which when overlaid onto a conventional ^{1}H image of the site (d) reveals PFOB and CE labeled cells localized to the left and right leg, respectively (dashed line indicates 3 × 3 cm^{2} field of view for ^{19}F images). (e, f) Similarly, at 1.5 T, ^{19}F image of ~4 × 106 CE-loaded cells (e) locates to the mouse thigh in a ^{1}H image of the mouse cross section (f). The absence of background signal in ^{19}F images (b, c, e) enables unambiguous localization of perfluorocarbon-containing cells at both 11.7 T and 1.5 T. (Reprinted with permission from Partlow *et al.*[40])

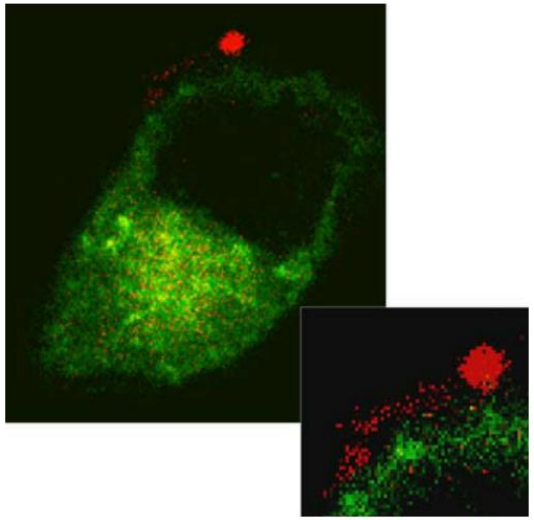

FIGURE 6. "Lipid streaming" into the plasma membrane. A high power image of a cell surface (see inset) shows a bound rhodamine-labeled nanoparticle (red) with adjacent lipid mixing into the plasma membrane of a cell transiently expressing a green cytoplasmic marker. The cellular features that can be observed are the nucleus (dark circular region), cell cytoplasm (green), and plasma membrane (directly adjacent to cell cytoplasm, only small portion is labeled with red lipid from nanoparticle). (Reprinted with permission from Crowder *et al.*[9])

A. The orthogonality of the fluorous phase **B. Previous work on fluorous fluorophores, "fluorofluorophores"**

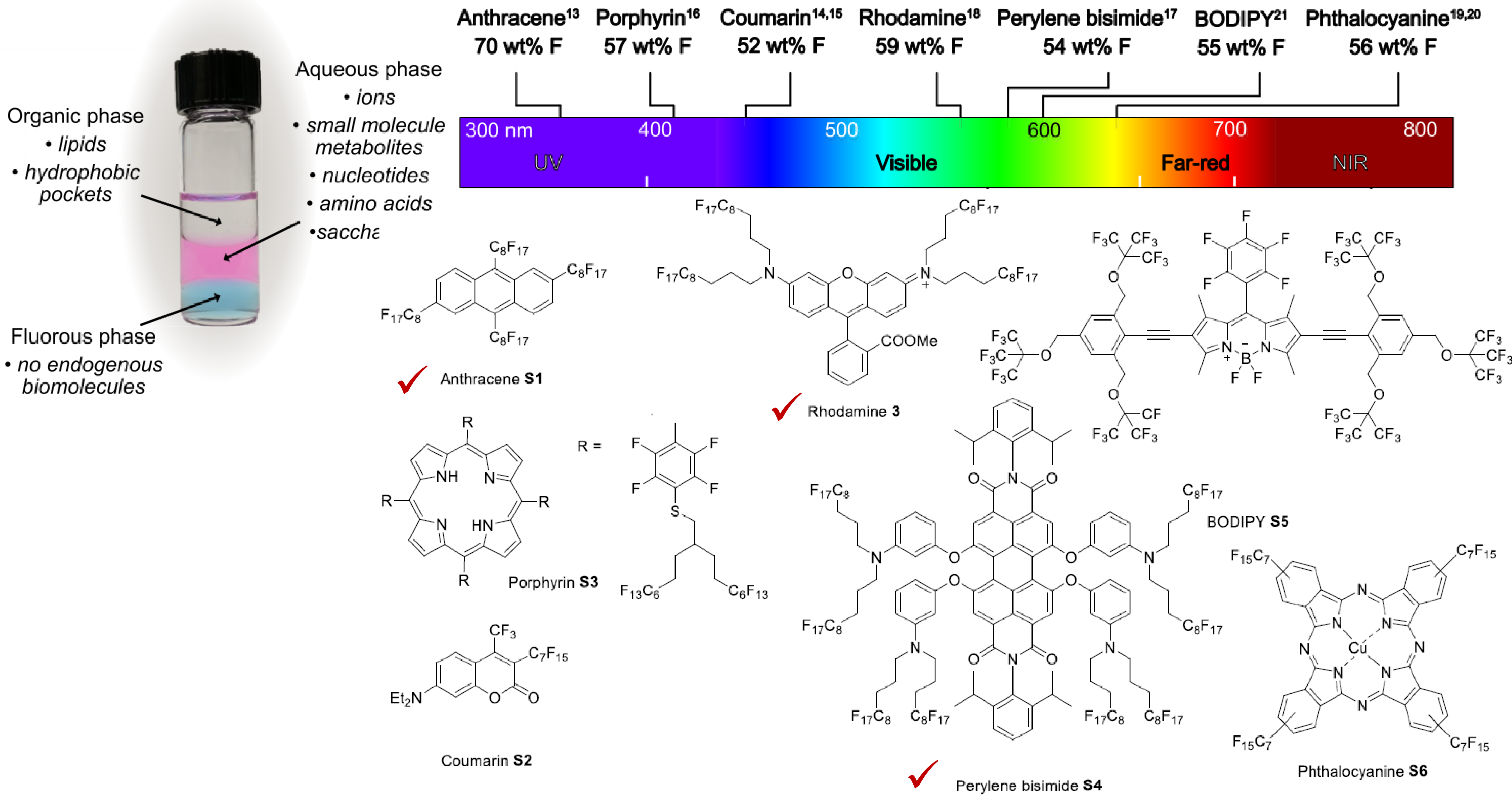

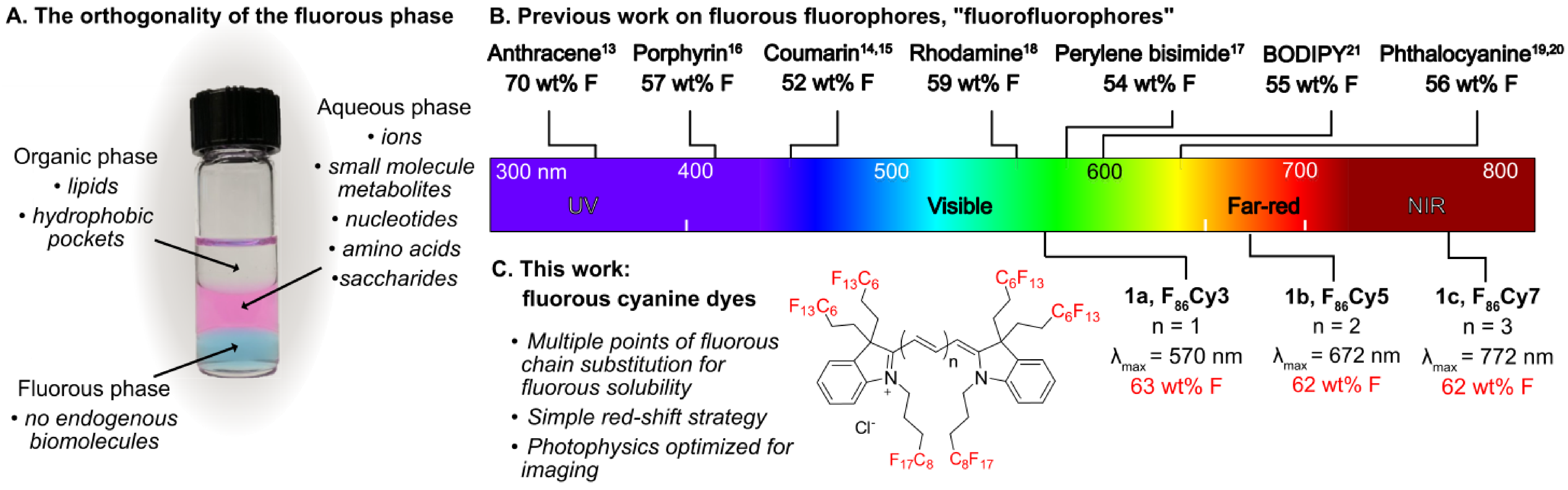

- ✓ The wt% F is minimally altered to implement a 100 nm shift
- ✓ The tags surround the chromophore when placed in fluorous solvent to maximize fluorous solubility
- ✓ Multichannel experiments

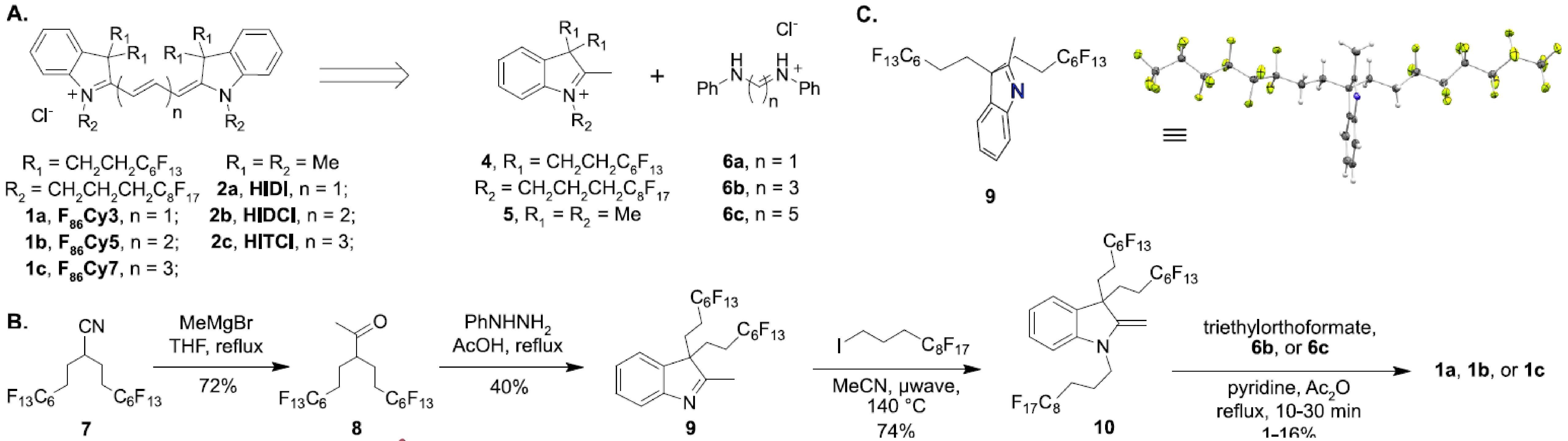

Organic LETTERS
Letter
Cite This: *Org. Lett.* 2018, 20, 6850–6854
pubs.acs.org/OrgLett

A General Approach to Biocompatible Branched Fluorous Tags for Increased Solubility in Perfluorocarbon Solvents

Margeaux A. Miller and Ellen M. Sletten*

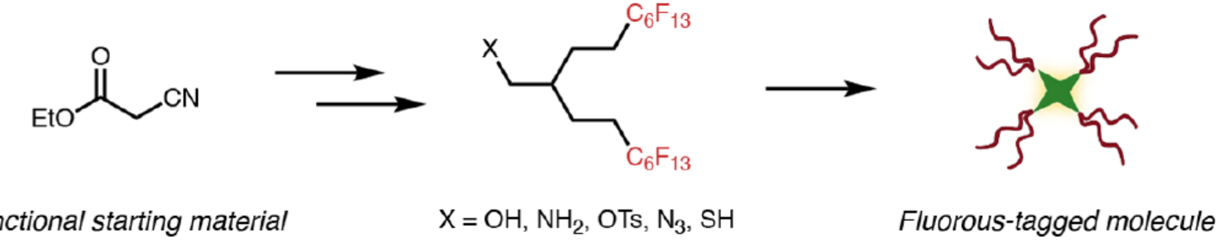

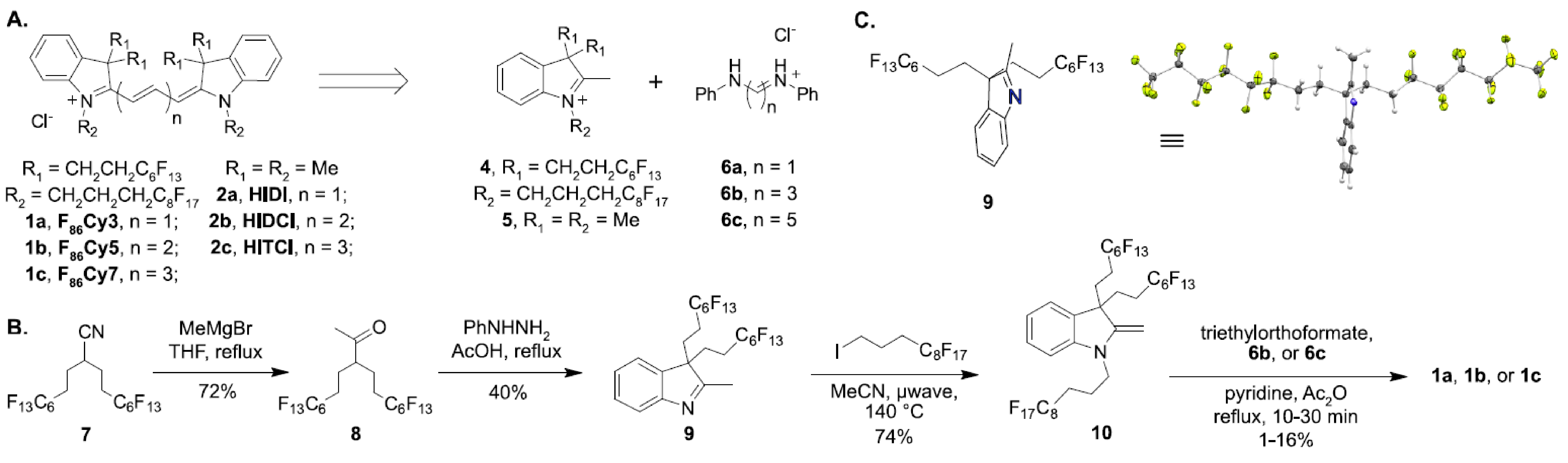

A.

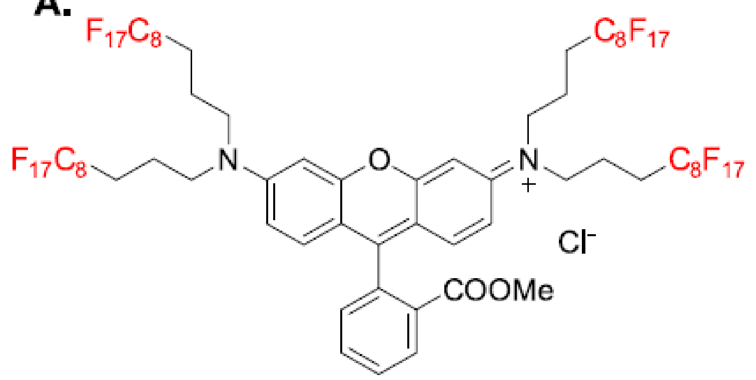

3, Fluorous Rhodamine

全氟甲基环己烷

B.

	$\log_F\left(\frac{PFMC}{Toluene}\right)$	Solubilities in acetone		Solubilities in PFMC	
		Abs (mM)	Relative	Abs (mM)	Relative
1a	1.82	0.91	10.7	0.12	11
1b	0.157	0.11	1.3	0.21	8
1c	2.35	0.09	1	0.04	3
3	1.42	0.15	1.7	0.01	1

C.

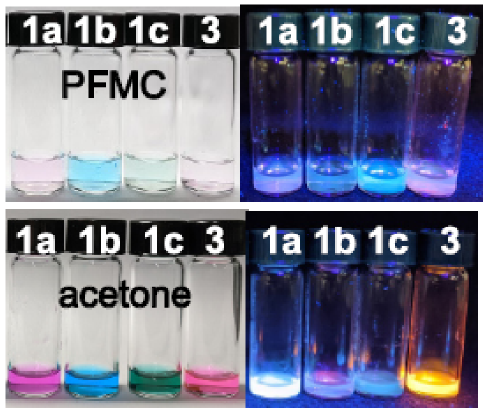

Visible UV

Impact of Fluorous Tags on Photophysical Properties

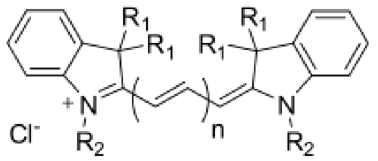

$R_1 = CH_2CH_2C_6F_{13}$
$R_2 = CH_2CH_2CH_2C_8F_{17}$
1a, **F_{86}Cy3**, n = 1;
1b, **F_{86}Cy5**, n = 2;
1c, **F_{86}Cy7**, n = 3;

$R_1 = R_2 = Me$
2a, **HIDI**, n = 1;
2b, **HIDCI**, n = 2;
2c, **HITCI**, n = 3;

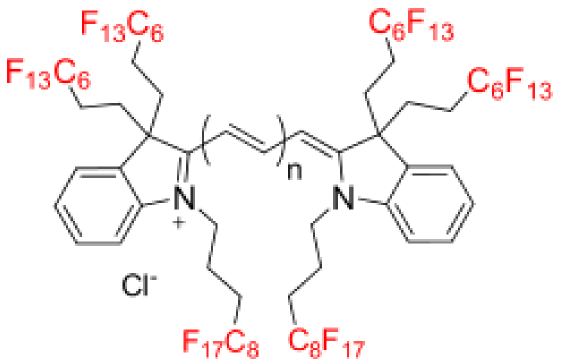

D.

Solvents	$\lambda_{max,abs}$ (nm) 1a	1b	1c	$\lambda_{max,em}$ (nm) 1a	1b	1c	ε (x 10^3 $M^{-1}cm^{-1}$) 1a	1b	1c	ϕ_F 1a	1b	1c
EtOH	570	656	758	588	682	790	38.3	228	180	0.115	0.291	0.16

EtOH	$\lambda_{max,abs}$ (nm)	$\lambda_{max,em}$ (nm)	ε (x 10^5 $M^{-1}cm^{-1}$)	Φ_F
2a	546	563 nm	0.60 x 10^5 $\pm$ 0.01	2.16% $\pm$ 0.07
2b	641	664 nm	1.19 x 10^5 $\pm$ 0.02	27.9% $\pm$ 0.3
2c	741	768 nm	1.73 x 10^5 $\pm$ 0.02	15.2% $\pm$ 0.8

D.

Solvents	$\lambda_{max,abs}$ (nm) 1a	1b	1c	$\lambda_{max,em}$ (nm) 1a	1b	1c	ε (x 10^3 $M^{-1}cm^{-1}$) 1a	1b	1c	ϕ_F 1a	1b	1c
acetone	571	655	762	591	677	792	105	182	199	0.109	0.573	0.20

acetone	$\lambda_{max,abs}$ (nm)	$\lambda_{max,em}$ (nm)	ε (x 10^5 $M^{-1}cm^{-1}$)	Φ_F
2a	545	563	0.53 $\pm$ 0.01	1.60% $\pm$ 0.01
2b	639	663	1.20 $\pm$ 0.02	11% $\pm$ 1
2c	741	766	1.61 $\pm$ 0.06	12.4% $\pm$ 0.7

F.

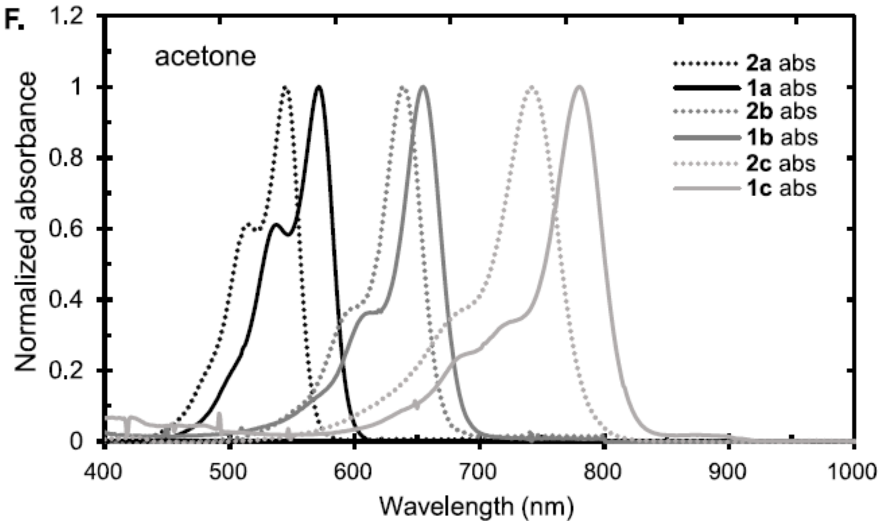

G.

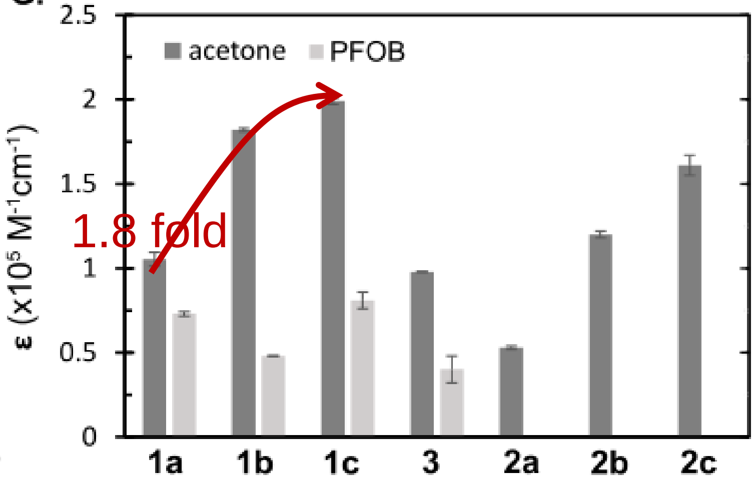

H.

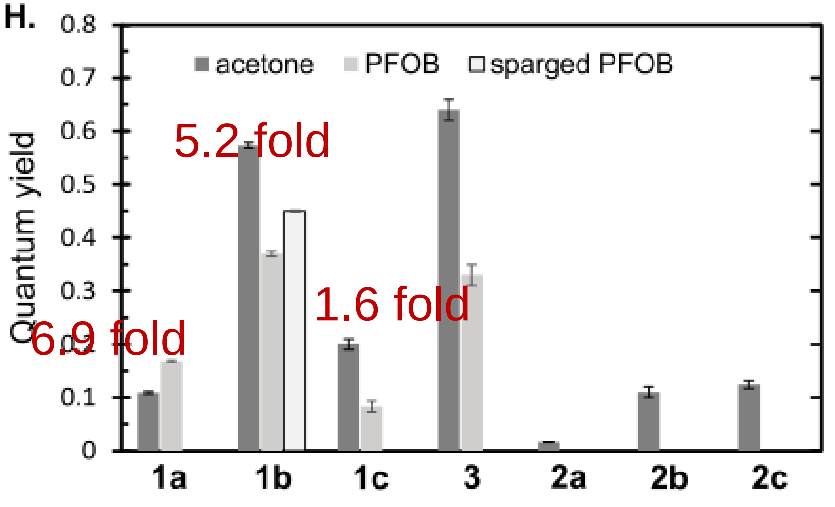

Impact of Fluorous Solvent on Photophysical Properties

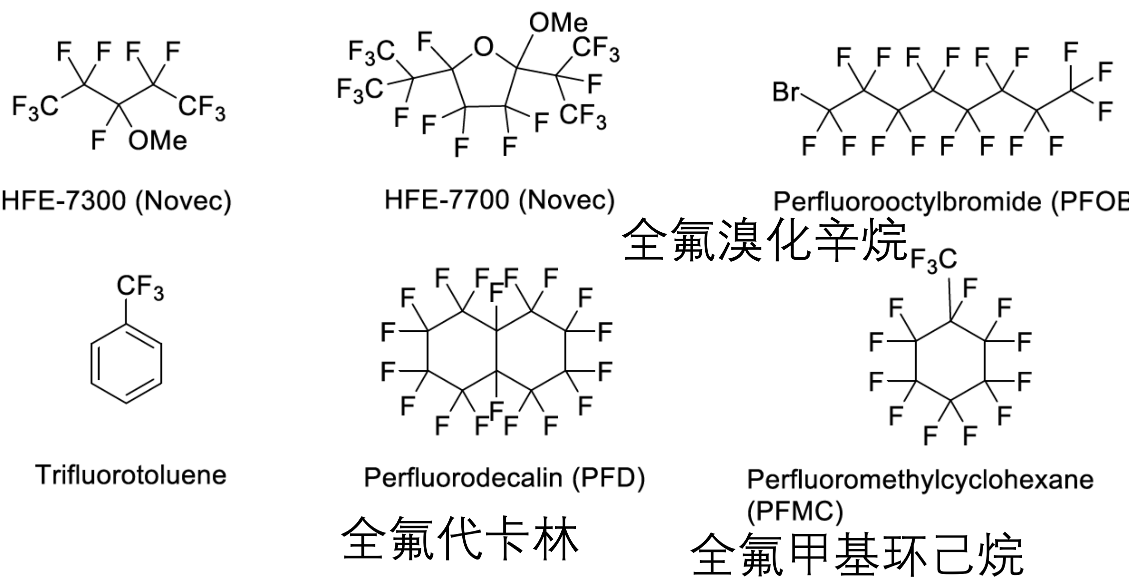

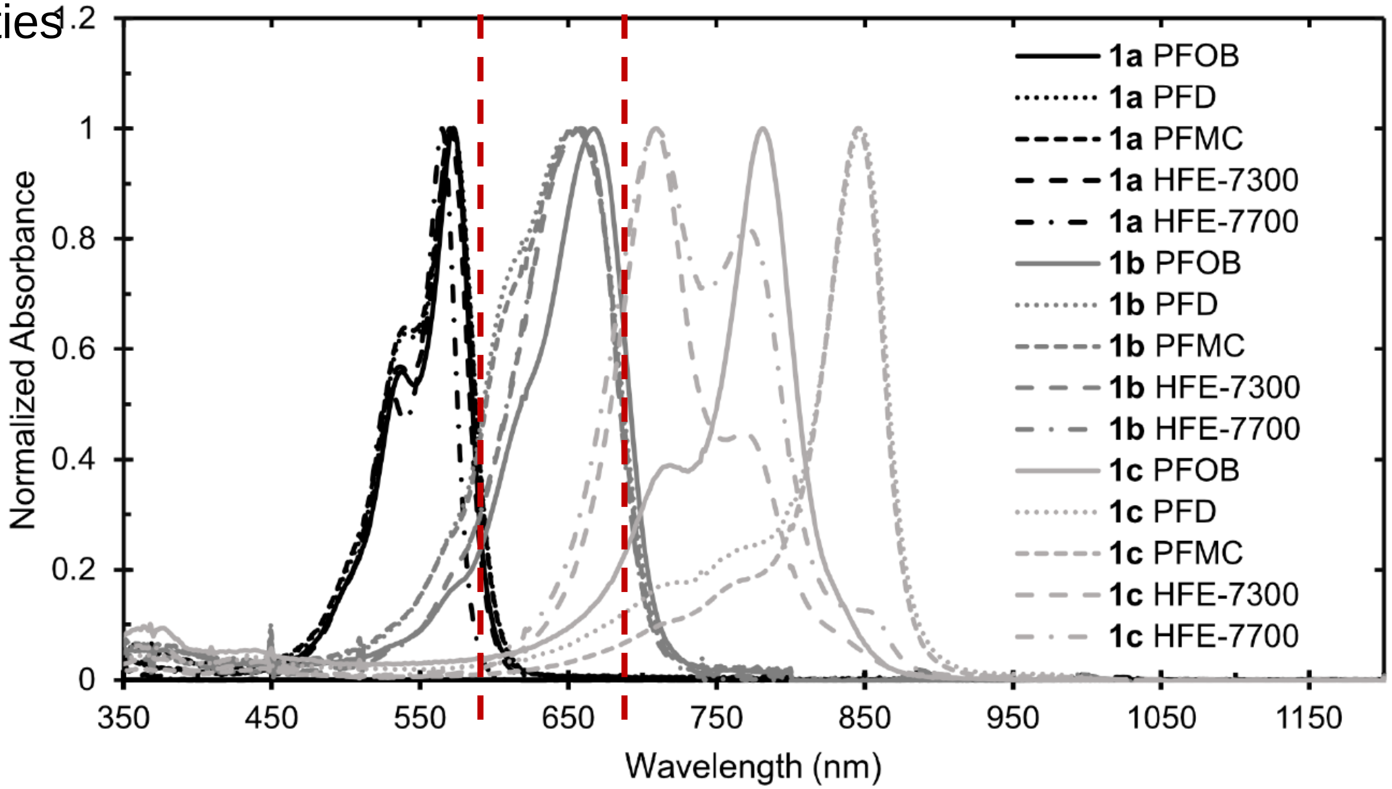

D.

Solvents	$\lambda_{max,abs}$ (nm)			$\lambda_{max,em}$ (nm)			ε (x 10³ $M^{-1}cm^{-1}$)			ϕ_F		
	1a	1b	1c	1a	1b	1c	1a	1b	1c	1a	1b	1c
EtOH	570	656	758	588	682	790	38.3	228	180	0.115	0.291	0.16
acetone	571	655	762	591	677	792	105	182	199	0.109	0.573	0.20
DCM	a	672	773	a	691	800	a	81	254	a	0.59	0.22
PFOB	572	668	781	584	694	800	73	48	81	0.17	0.37	0.083
PFMC	571	659	845	581	688	b	27	27	c	0.044	0.24	b
PFD	572	658	848	582	690	b	30	27	c	0.024	0.37	b
HFE-7300	570	659	772	584	685	787	c	32	c	0.095	0.33	0.035
HFE-7700	565	658	772	576	690	787	c	30	c	0.049	0.55	0.11

70-80%

50-70%

a Not soluble b No emission c Not obtained

Impact of Fluorous Solvent on Photophysical Properties

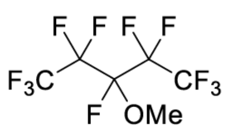

HFE-7300 (Novec)

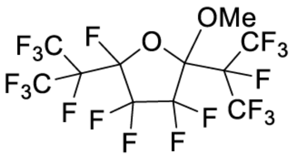

HFE-7700 (Novec)

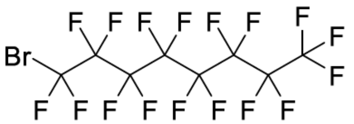

Perfluorooctylbromide (PFOB

全氟溴化辛烷

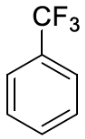

Trifluorotoluene

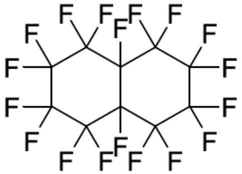

Perfluorodecalin (PFD)

全氟代卡林

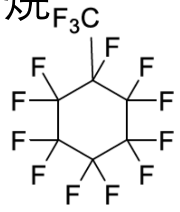

Perfluoromethylcyclohexane (PFMC)

全氟甲基环己烷

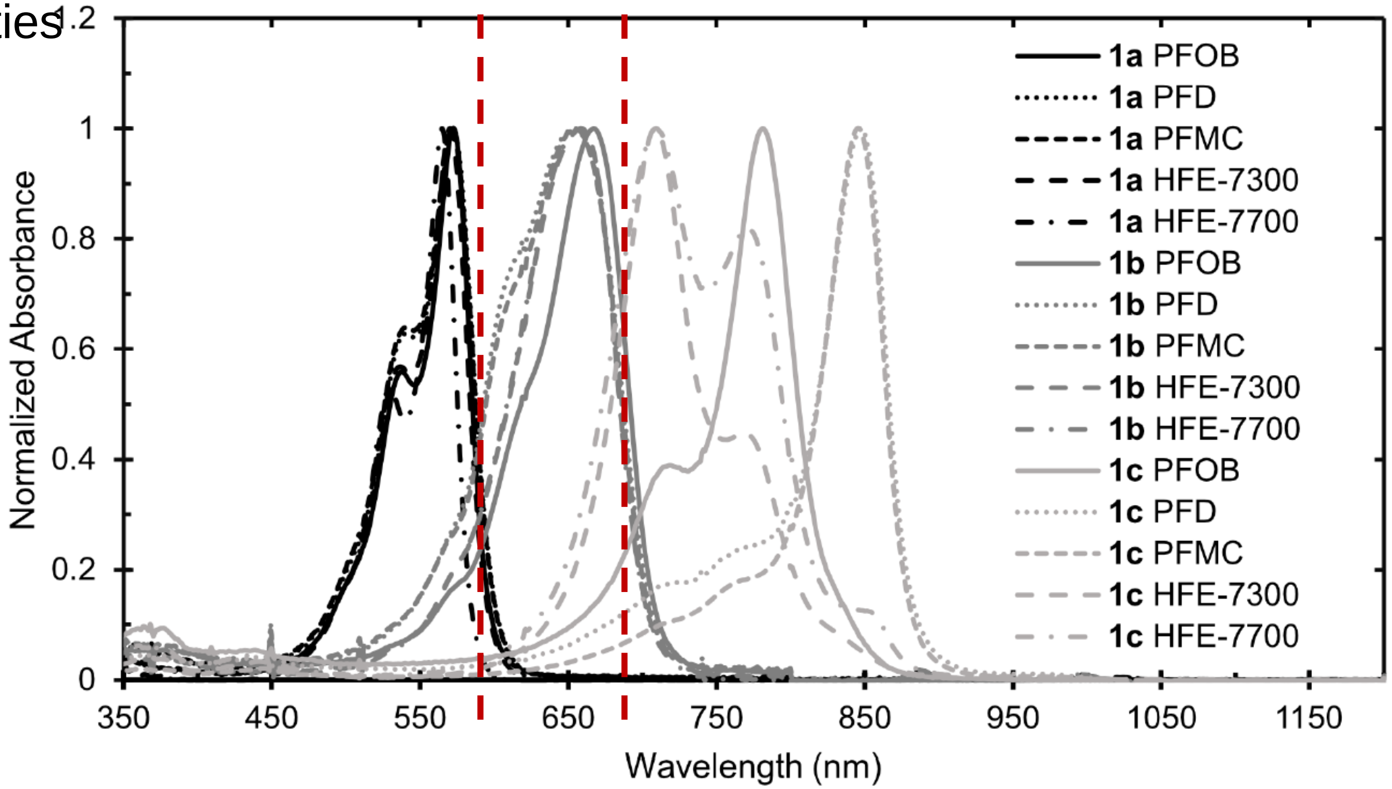

D.

Solvents	$\lambda_{max,abs}$ (nm)			$\lambda_{max,em}$ (nm)			ε (x 10^3 $M^{-1}cm^{-1}$)			ϕ_F		
	1a	1b	1c	1a	1b	1c	1a	1b	1c	1a	1b	1c
EtOH	570	656	758	588	682	790	38.3	228	180	0.115	0.291	0.16
acetone	571	655	762	591	677	792	105	182	199	0.109	0.573	0.20
DCM	a	672	773	a	691	800	a	81	254	a	0.59	0.22
PFOB	572	668	781	584	694	800	73 30%	48 73%	81 59%	0.17	0.37	0.083
PFMC	571	659	845	581	688	b	27	27	c	0.044	0.24	b
PFD	572	658	848	582	690	b	30	27	c	0.024	0.37	b
HFE-7300	570	659	772	584	685	787	c	32	c	0.095	0.33	0.035
HFE-7700	565	658	772	576	690	787	c	30	c	0.049	0.55	0.11

a Not soluble b No emission c Not obtained

Impact of Fluorous Tags and Fluorous Solvent on Photostability

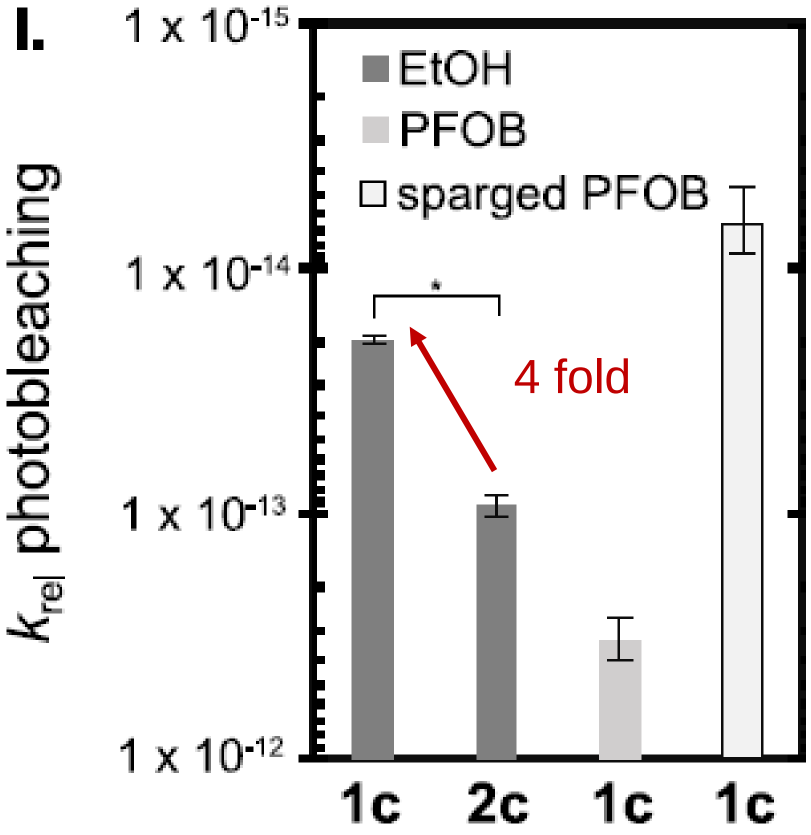

Solvent	Dye	log(k_{rel})
EtOH	**1a**	0
	1c	13.706
	2c	13.589
	3	15.8
PFOB	**1a**	14.76
	1b	13.26
	1c	12.4773
	3	15.10
O_2-free PFOB	**1a**	15.589
	1c	14.1816

Fluorescent Perfluorocarbon Nanoemulsions

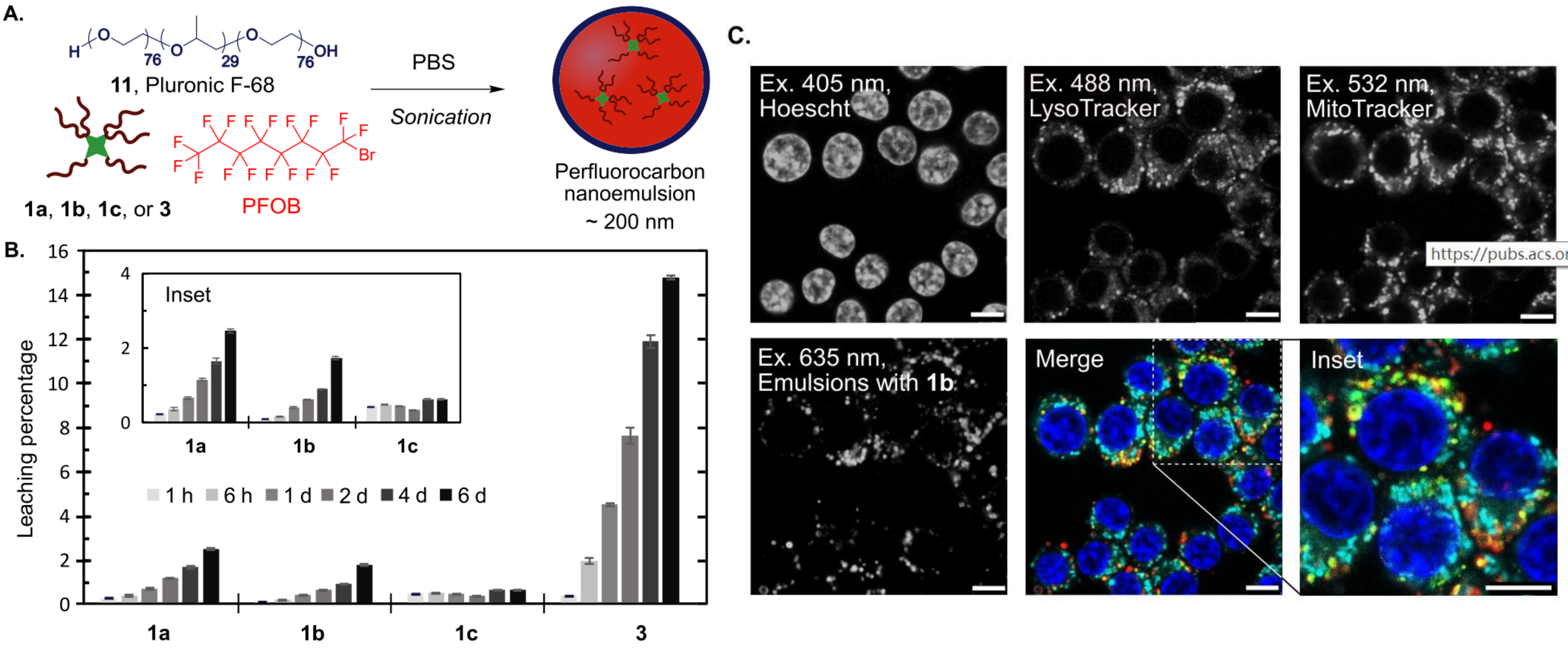

Force Measurements in Multicellular Aggregates and Zebrafish Tissues